Some Current Interatomic Potential Applications at Sandia

Atomistic Simulations for Industrial Needs

August 1 – 3, 2018, Rockville, MD

X. W. Zhou, R. B. Sills, M. E. Foster, and R. E. Jones

Sandia National Laboratories, USA

Sandia National Laboratories is a multi-mission laboratory managed and operated by National Technology and Engineering Solutions of Sandia, LLC., a wholly owned subsidiary of Honeywell International, Inc., for the U.S. Department of Energy's National Nuclear Security Administration under contract DE-NA-0003525. The views expressed in the article do not necessarily represent the views of the U.S. Department of Energy or the United States Government.

Outline

1. **Metal (e.g., Fe-Ni-Cr) embedded atom method potential[1]**
   - ➢ Suitable for close packed structures
2. **Semiconductor (e.g., In-Ga-N) Stillinger-Weber potential[2]**
   - ➢ Suitable for tetrahedral structures
4. **Al-Cu-H bond order potential[3]**
   - ➢ Suitable for compounds

(1) Zhou et al, to be published; **(2)** Zhou et al, PRB, 88, 085309 (2013); **(3)** Zhou et al, NJC, 42, 5215 (2018).

Fe-Ni-Cr-H embedded-atom method (EAM) potential ……

Five criteria of high-fidelity Fe-Ni-Cr interatomic potential

1. give reasonable energy and volume for various compositions
2. permit stable high temperature MD simulations
3. prescribe well the elastic constants
4. capture the correct stacking fault energy (γ_{sf})
5. pass stringent MD validation tests

Status of literature potentials

1. The potential we published (CALPHAD 1993, 17, 383) did not consider the four criteria
2. Smith and Was' potential (PRB 1989, 40, 10322) was fitted to effective atoms and did not consider stacking fault energy
3. The 2013 version of Bonny et al's potential (MSMSE 2013, 21 085004) predicts phase separation

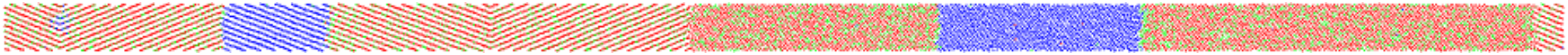

4. The 2011 version of Bonny et al's potential (MSMSE 2011, 19, 085008) predicts negative slope of stacking fault energy with Ni composition
5. Tong et al's potential (Mol. Sim. 2016, 42, 1256) predicts large negative stacking fault energy (~ -200 mJ/m^2)

Energy and volume trends

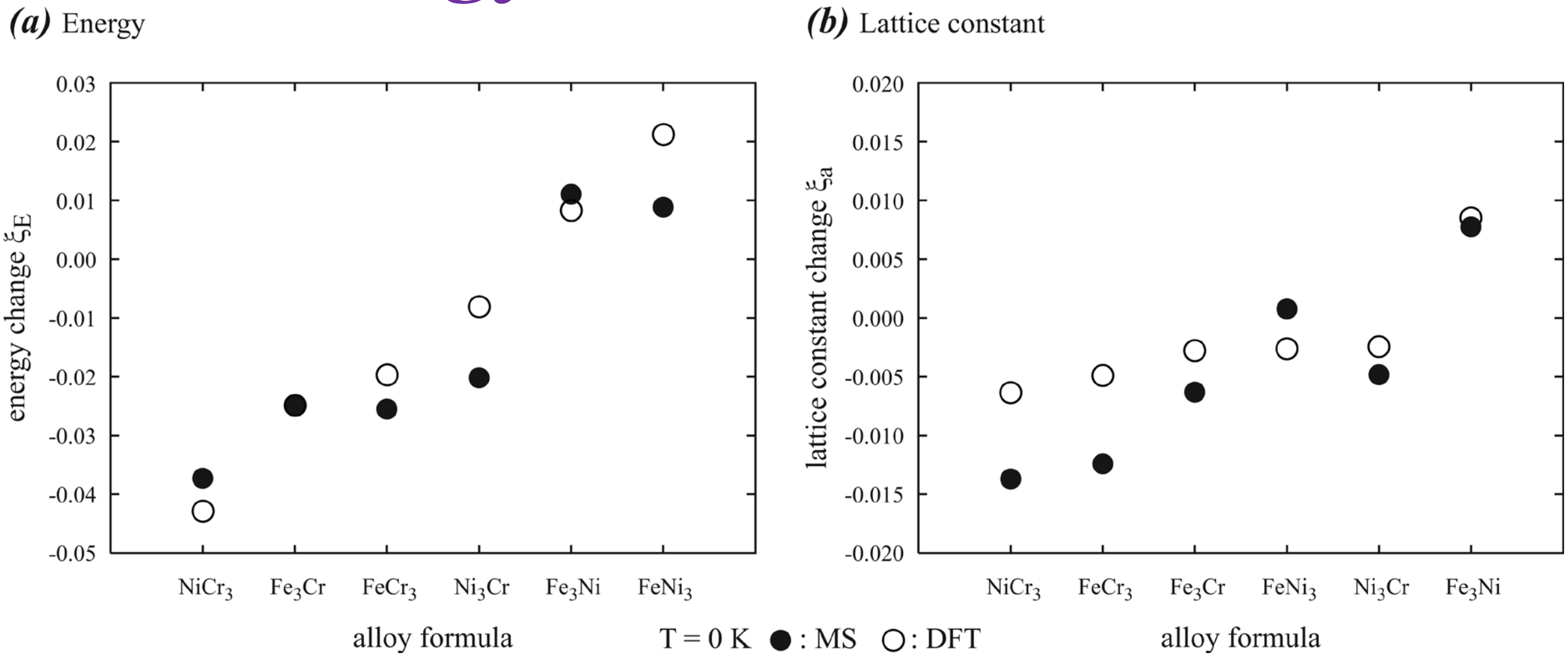

Calculated welling parameters for Ni and Cr in bcc Fe are 10% and 8% respectively, compared to 5% and 4% experimental values (King, J. Mater. Sci., 1, 79, 1966)

Heats/Gibbs free energy of solution

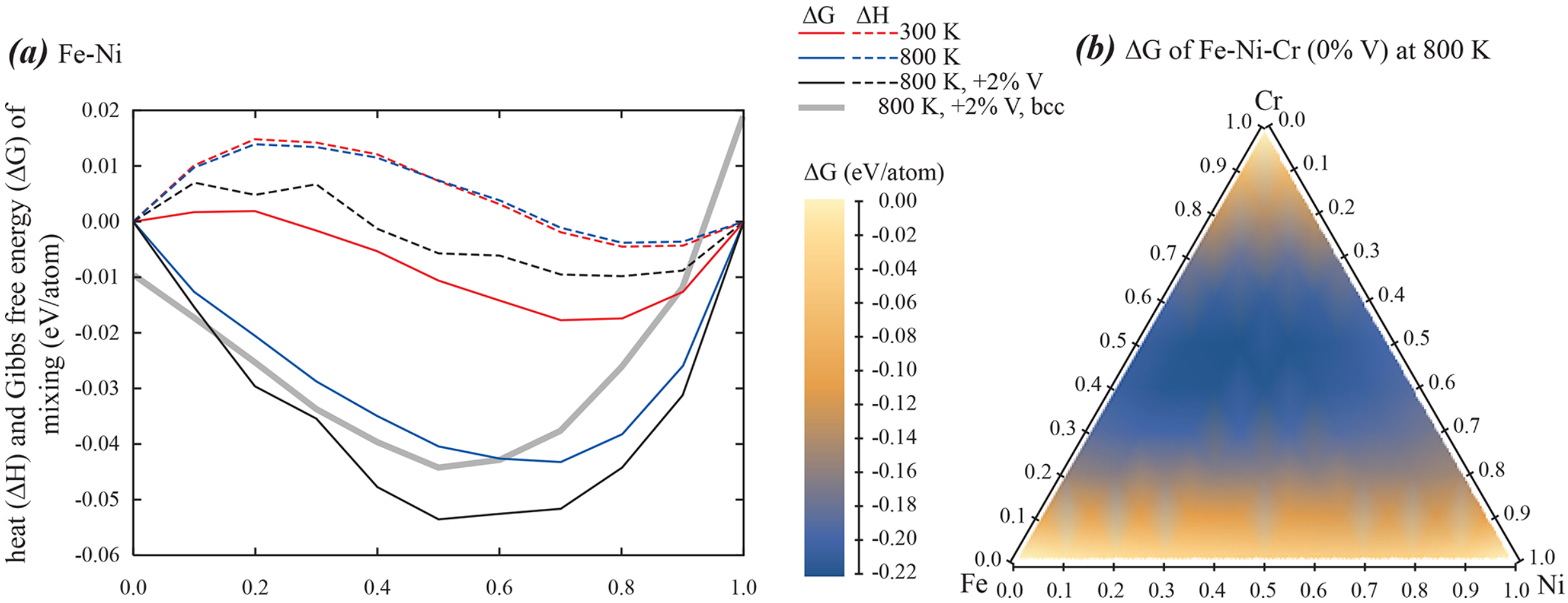

Elastic constants

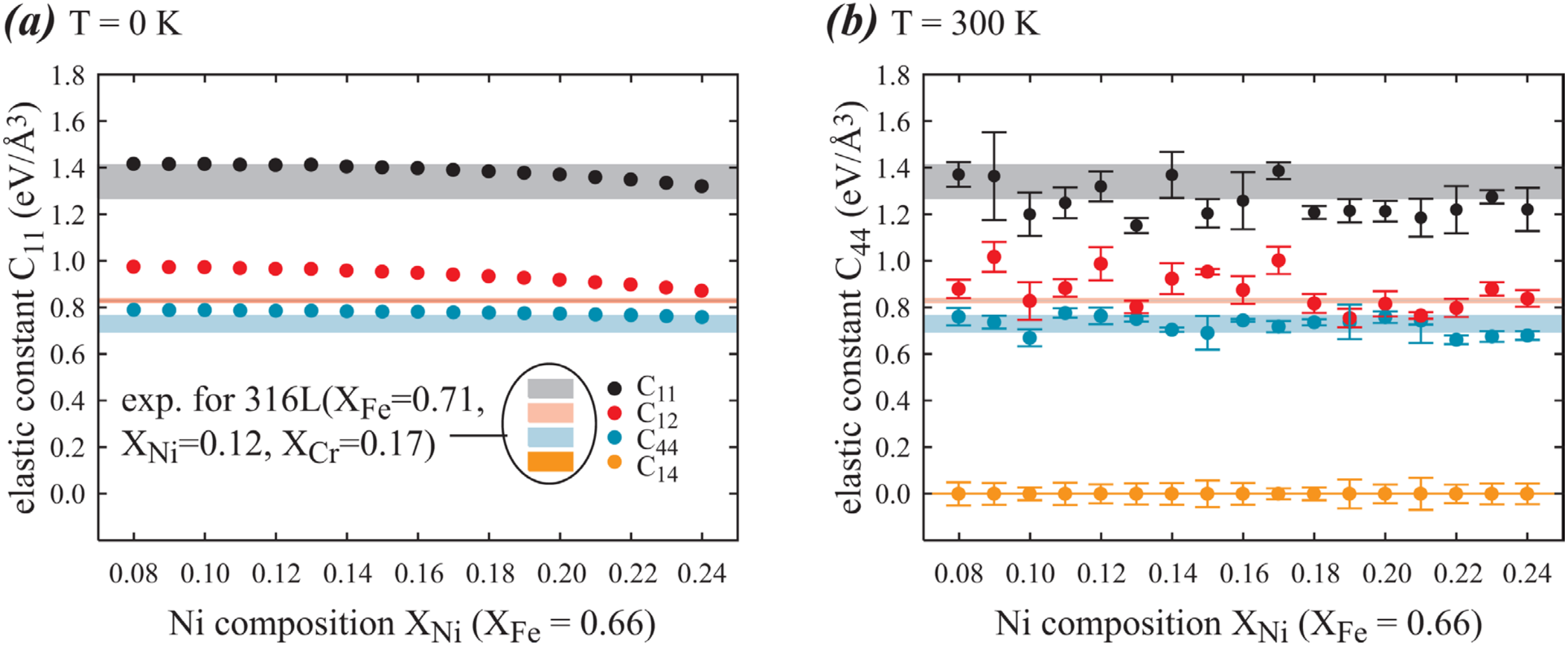

Experimental data for 316L from **(1)** Ledbetter, Ultrasonics 1985, 23, 9; **(2)** Bonny et al, MSMSE 2011, 19, 085008; **(3)** Bonny et al, MSMSE 2013, 21, 085004.

area ~ 1000 nm^2

Stacking fault energy

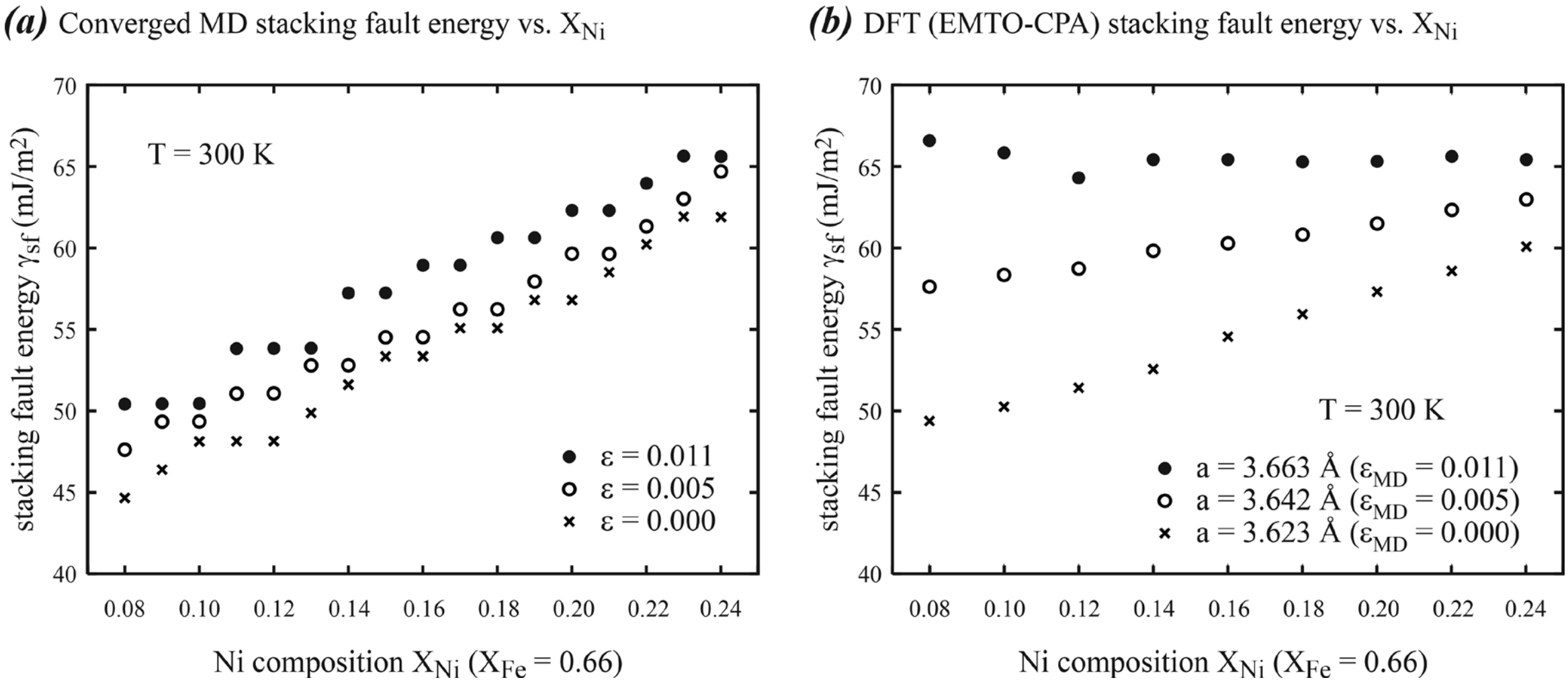

The predicted stacking fault energies match well with experimental results (see, for example, Vitos et al, PRL 2006, 96, 117210, and references therein).

Melting

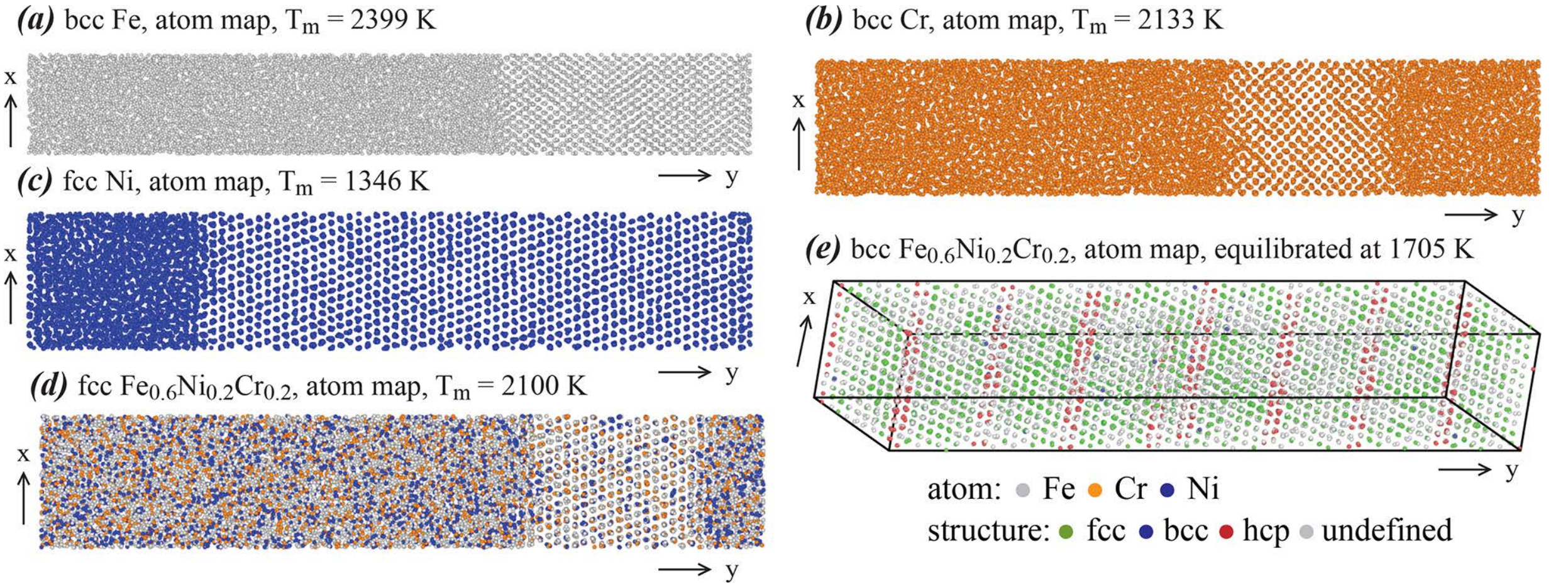
(a) bcc Fe, atom map, T_m = 2399 K
x
y
(b) bcc Cr, atom map, T_m = 2133 K
x
y
(c) fcc Ni, atom map, T_m = 1346 K
x
y
(d) fcc $Fe_{0.6}Ni_{0.2}Cr_{0.2}$, atom map, T_m = 2100 K
x
y
(e) bcc $Fe_{0.6}Ni_{0.2}Cr_{0.2}$, atom map, equilibrated at 1705 K
x
y
atom: Fe Cr Ni
structure: fcc bcc hcp undefined

Growth simulations

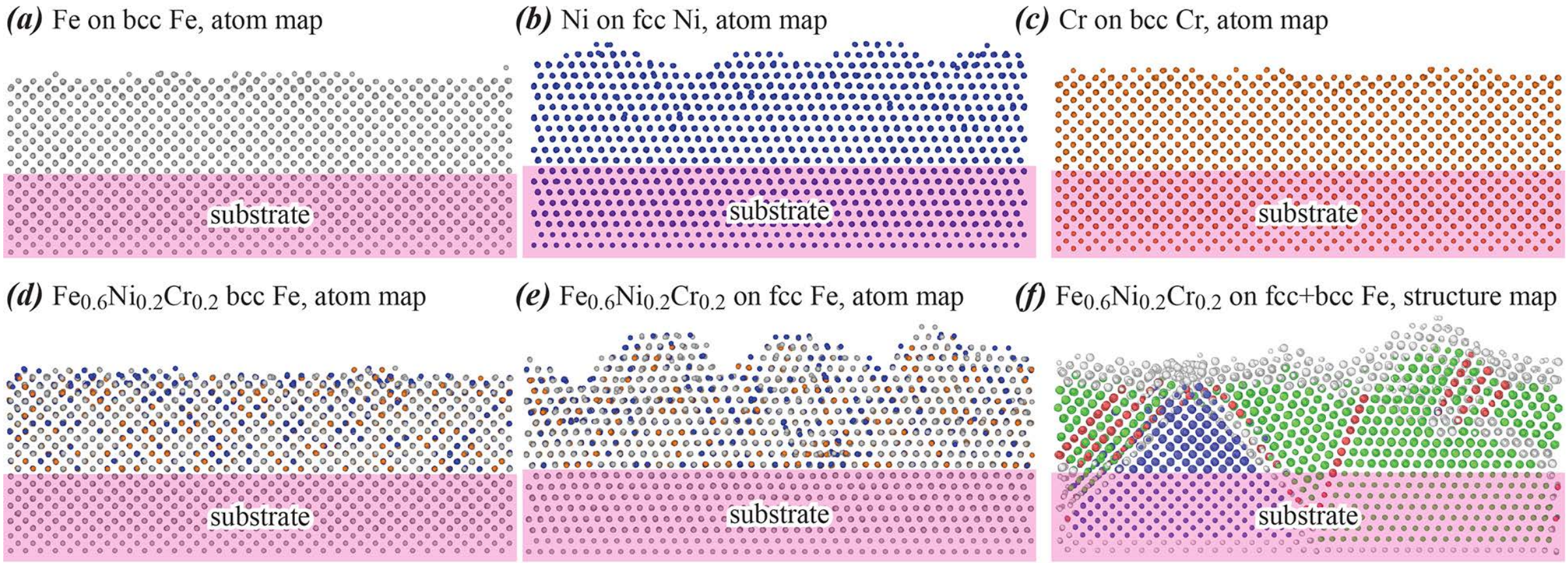

Semiconductor Stillinger-Weber (SW) potential ……

InGaN/GaN misfit dislocation

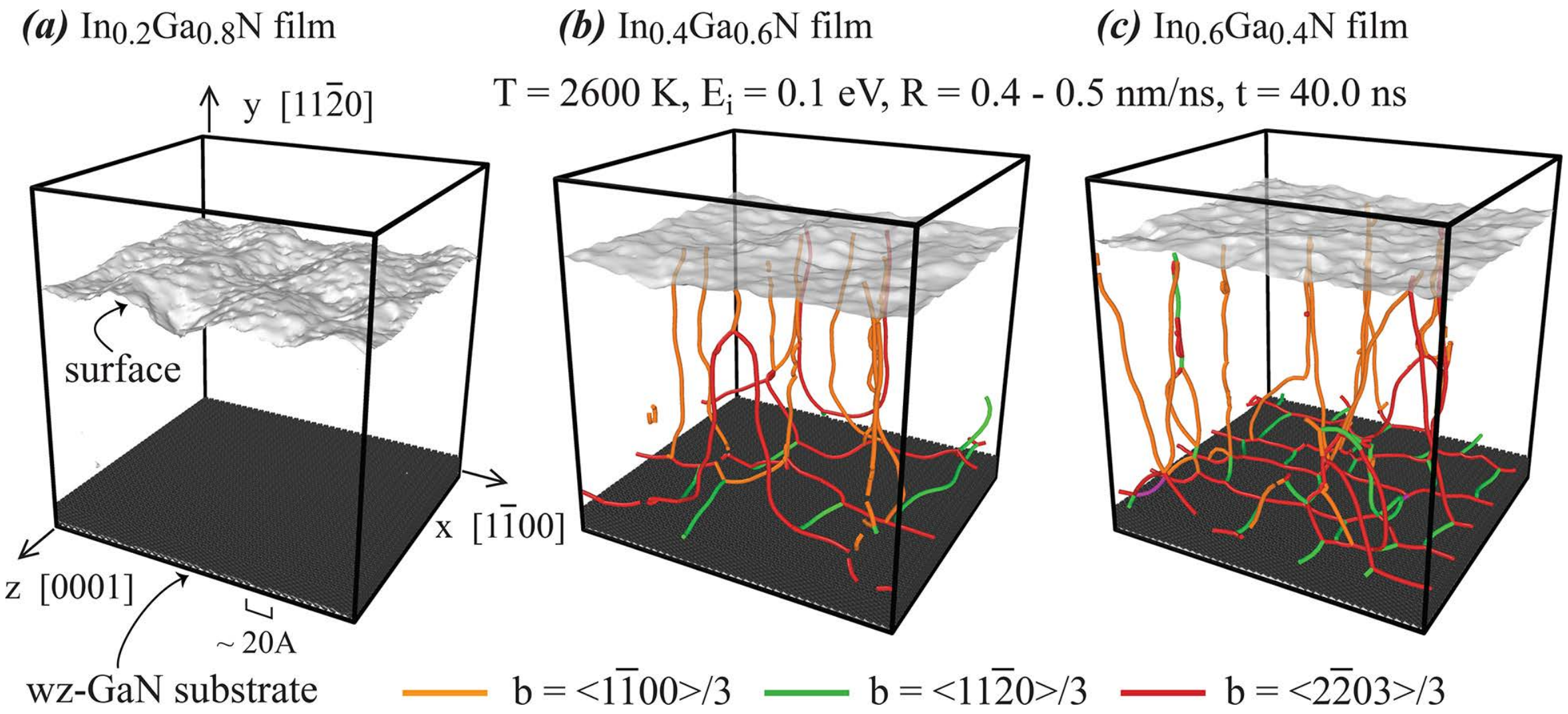

Chu et al, PRM, 2, 013402 (2018)

Growth simulations challenging

- Random condensation of adatoms leads to amorphous structures

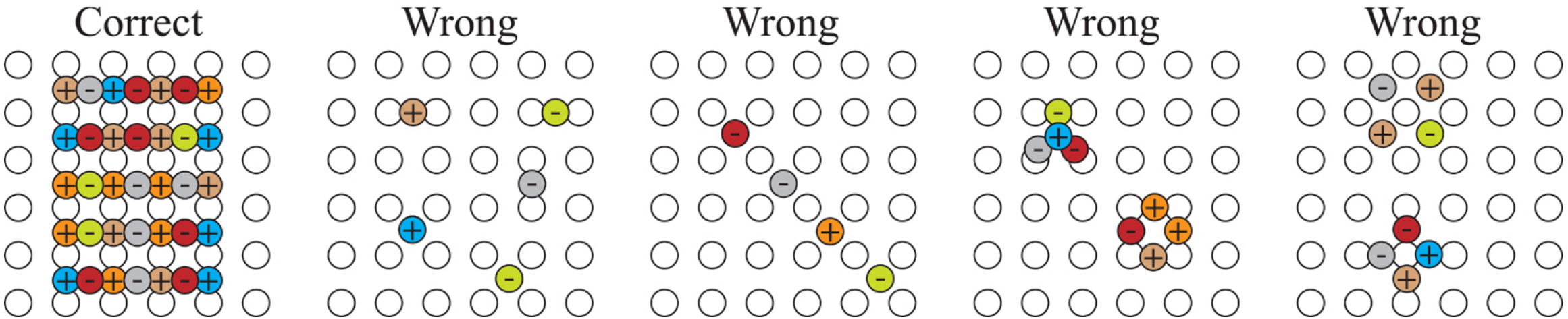

- The equilibrium phase must be more stable than ANY OTHER structures

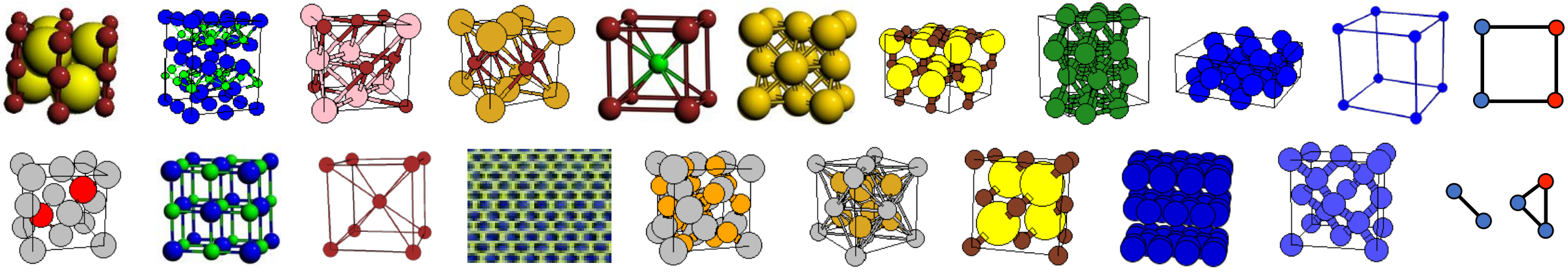

SW potential format

$$E = \frac{1}{2}\sum_{i=1}^{N}\sum_{j=i_1}^{i_N}\left[V_{IJ}^{R}\left(r_{ij}\right) - V_{IJ}^{A}\left(r_{ij}\right) + u_{IJ}\left(r_{ij}\right)\sum_{\substack{k=i_1 \\ k\neq j}}^{i_N} u_{IK}\left(r_{ik}\right)\left(\cos\theta_{jik} + \frac{1}{3}\right)^2 \right]$$

- $i_1, i_2, \ldots, i_N$, a list of all i's neighbors
- $V^R_{IJ}(r)$, $V^A_{IJ}(r)$, $u_{IJ}(r)$ are pair functions
- θ_{jik}: bond angle
- Easily ensure stability of tetrahedral structures

Two criteria of SW potential

1. Capture the lowest energy for the equilibrium phases to be studied
2. Best optimize the other properties

SW potential database

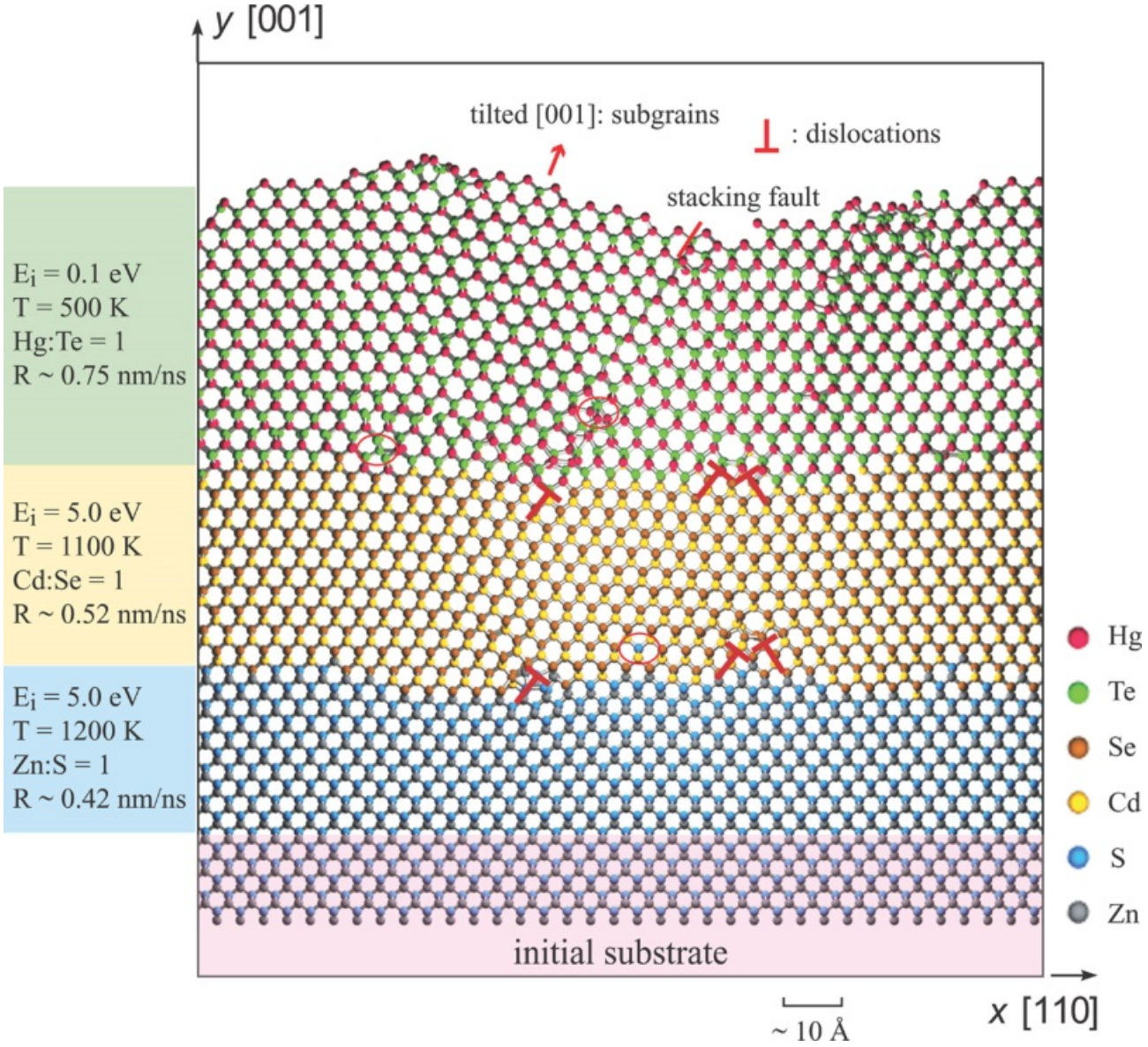

Example: Zn-Cd-Hg-S-Se-Te, Zhou et al, PRB, 88, 085309 (2013)

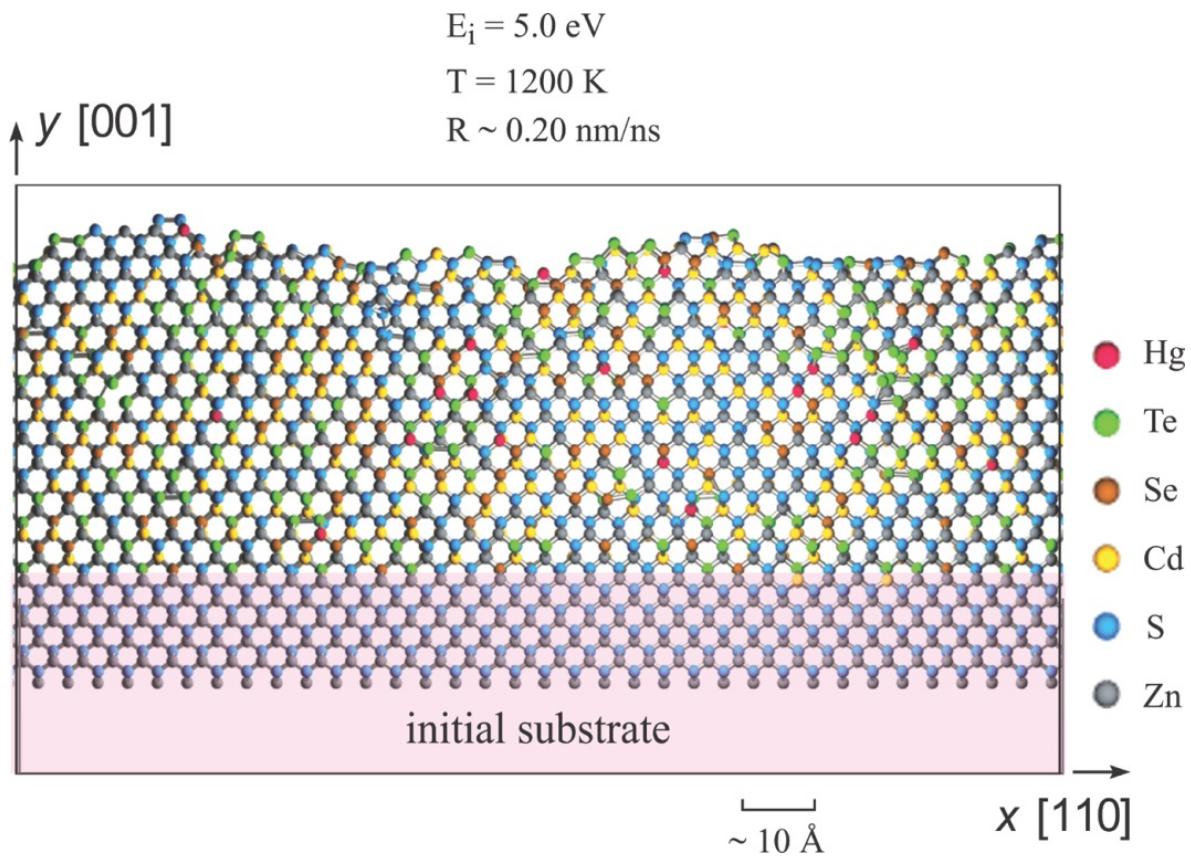

Low flexibility on property trends

Cd, Te energy trends

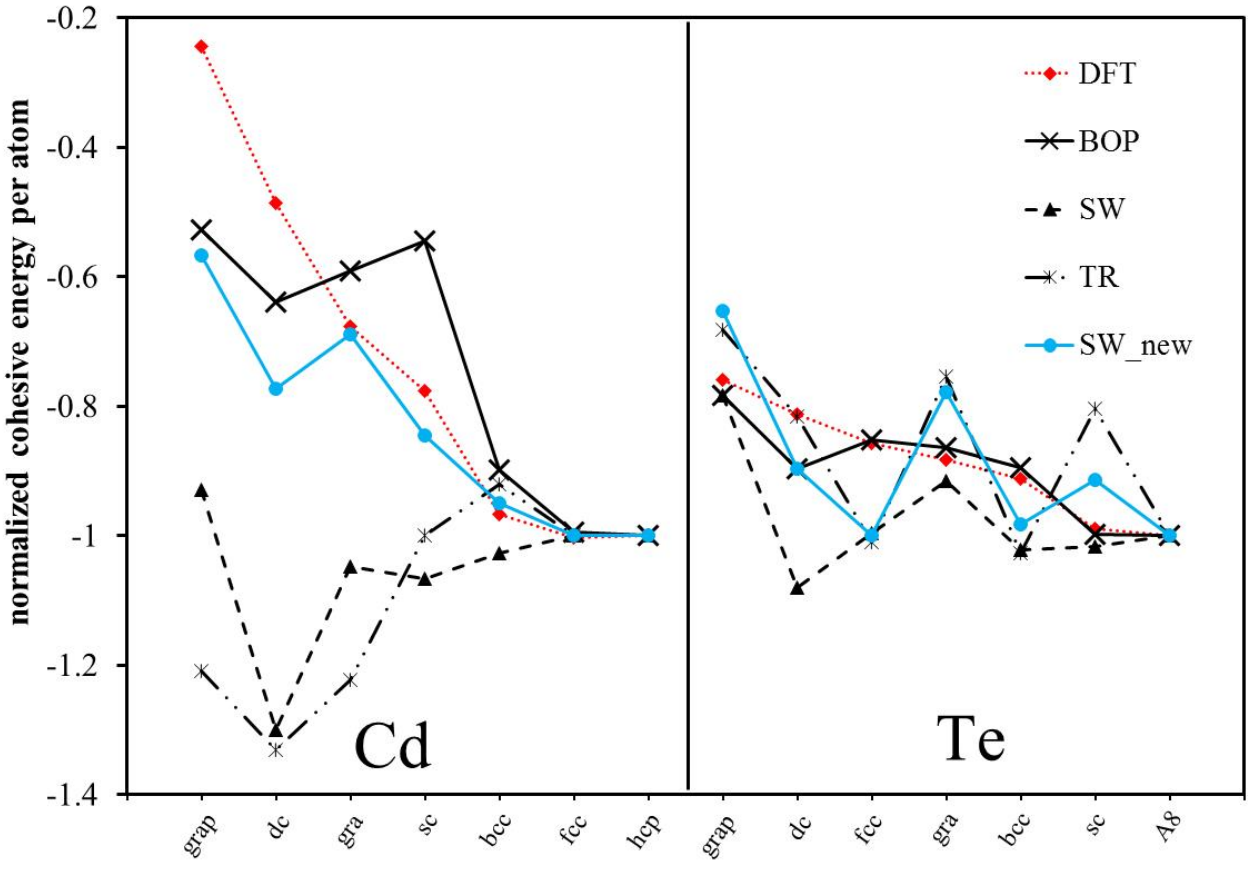

Cd-Te energy trends

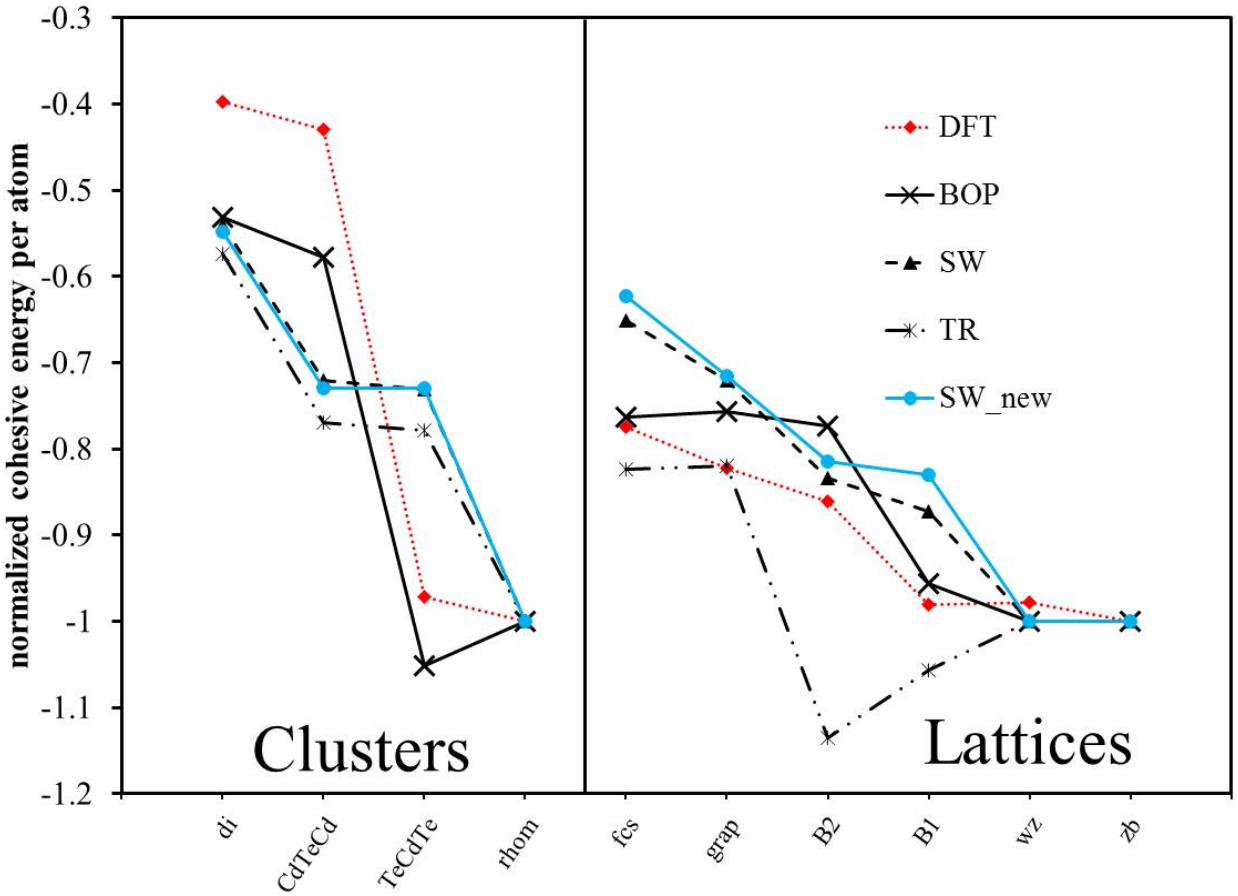

Al-Cu-H analytical bond order potential (BOP) ……

1. X. W. Zhou, D. K. Ward, and M. E. Foster, J. Alloys Compds. 2016, 680, 752;
2. X. W. Zhou, D. K. Ward, M. Foster, J. A. Zimmerman, J. Mater. Sci., 2015, 50, 2859.

Six criteria of high-fidelity Al-Cu-H interatomic potential

1. A high stacking fault energy of Al observed in experiments
2. Properties trends of a variety of stable and metastable structures
3. A positive heat of solution of Cu in Al
4. H2 $\Leftrightarrow$ 2H chemical reaction
5. $Al_{1-x}H_x \rightarrow Al + H_2$ and $Cu_{1-x}H_x \rightarrow Cu + H_2$ phase separations
6. Robust MD simulations of Al-rich side of the Al-Cu phase diagram

Status of literature potentials

Al stacking fault energy γ_{sf}

Model/Exp.	γ_{sf}
EAM-CY	1
EAM-Mishin1	141
EAM-BAM	85
EAM-VC	71
EAM-MSAH	126
EAM-Zhou	44
EAM-MKBA	125
EAM-JNP	0
MEAM	141
REAX-LJGS	0
REAX- Ojwang	1
Our BOP	133
Exp.	120-144,135

1. Many literature potentials do not capture high Al γ_{sf}
2. Many literature potentials do not capture θ, θ' Al_2Cu phases
3. Heat of solution of Cu in Al was misinterpreted
4. Most literature potentials do not capture $H_2 \Leftrightarrow 2H$, and Al + H_2 and Cu + H_2 phase separation
5. Robust MD validation tests were not passed

(a) Al-Cu phase diagram

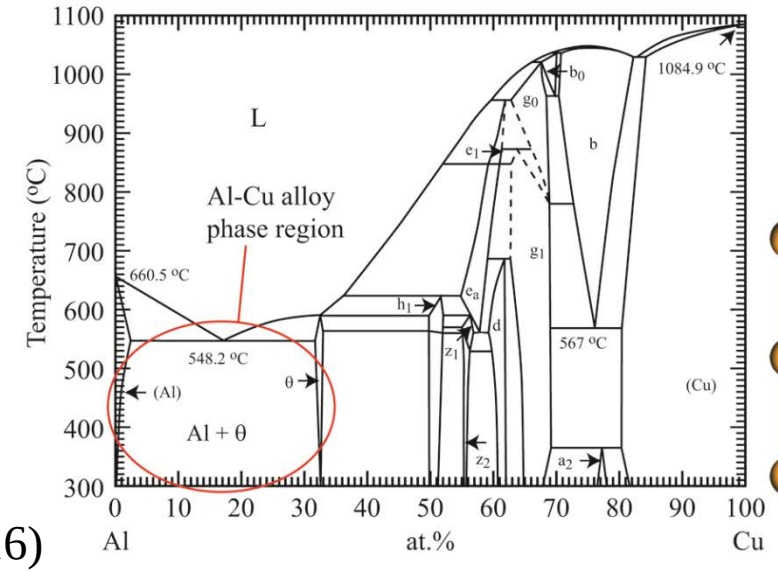

(b) crystal structure of the θ and θ' phases

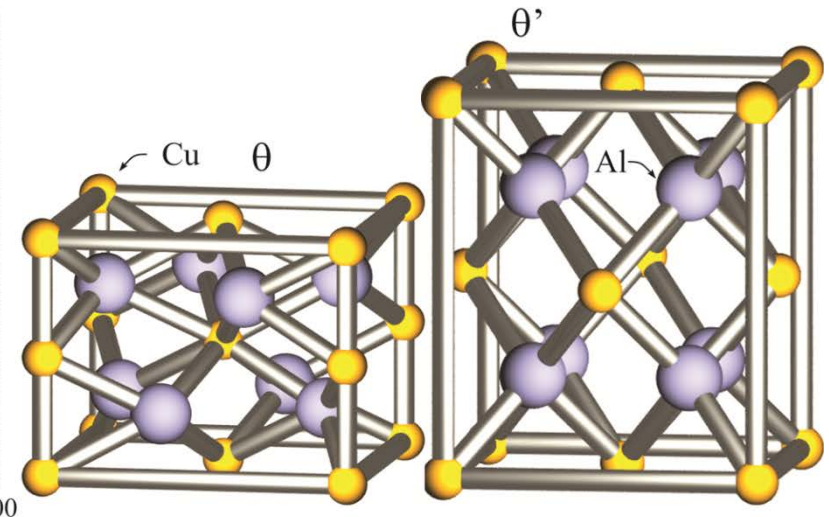

Zhou et al, J. Alloys Compds. 680, 752 (2016)

Energy and Volume Trends

Al, Cu, and Al-Cu

(a) cohesive energy E_c

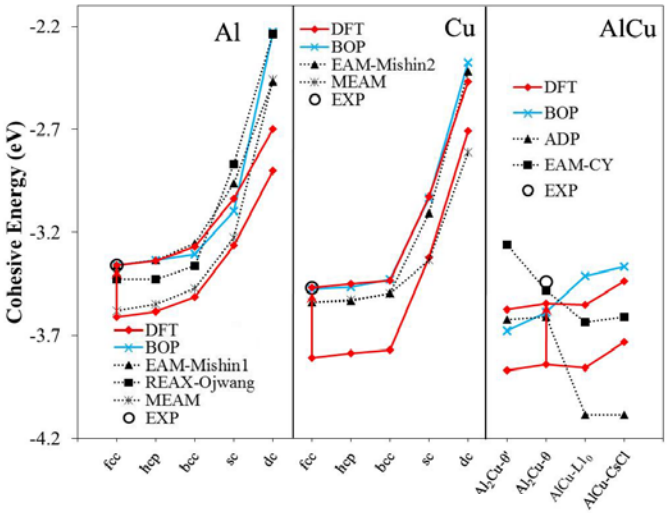

(b) atomic volume Ω

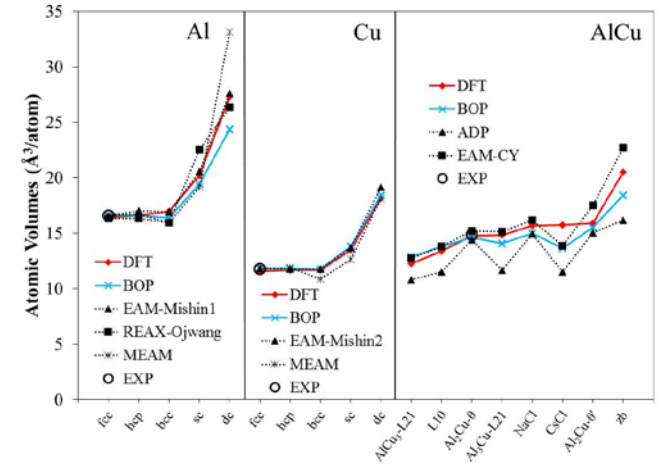

Cu-H

(a) cohesive energy E_c

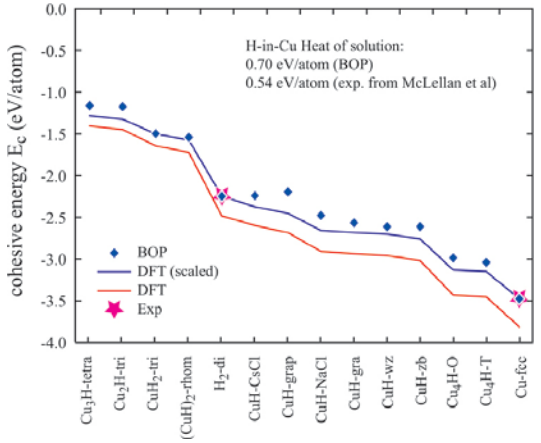

(b) atomic volume Ω

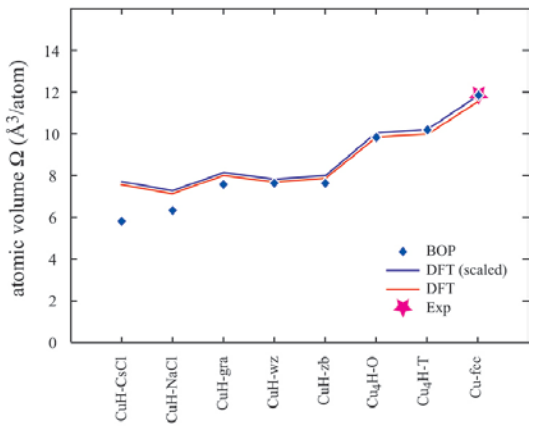

Al-H

(a) cohesive energy E_c

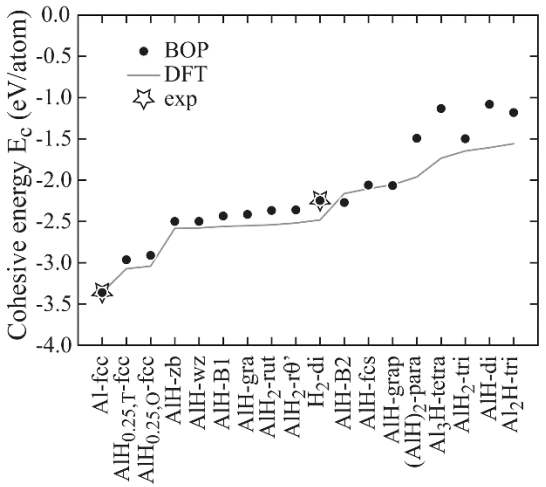

(b) atomic volume Ω

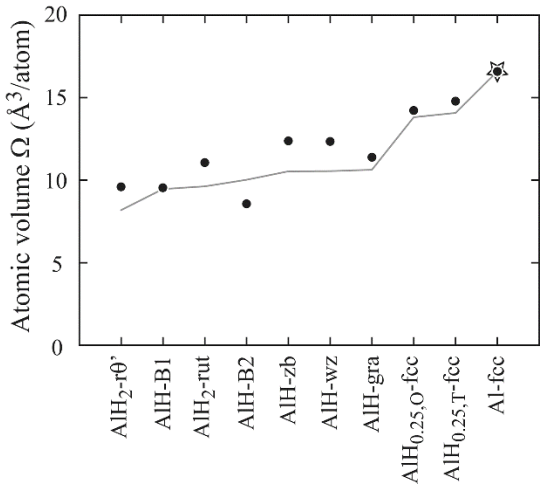

Heat of Solution

Al-Cu

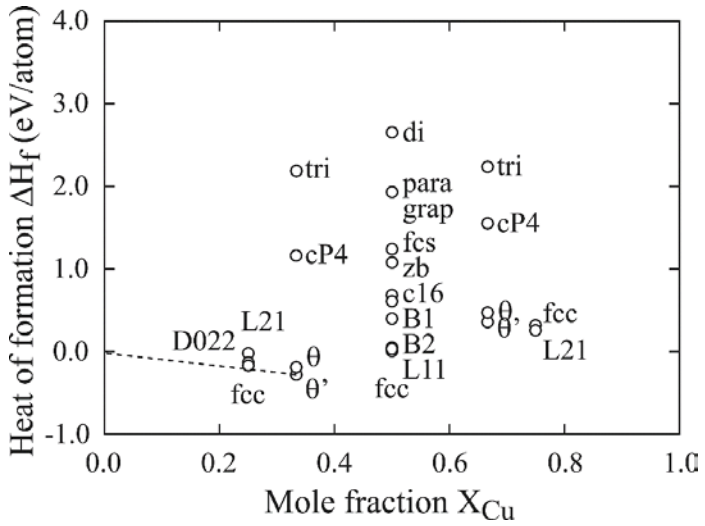

1. Energy and volume trends by potential matches well with those by DFT
2. Heat of solution supports stabilities of θ and θ' Al_2Cu phases

Dilute heat of solution ΔE_{ds} of Cu in Al

Al-Cu phase diagram

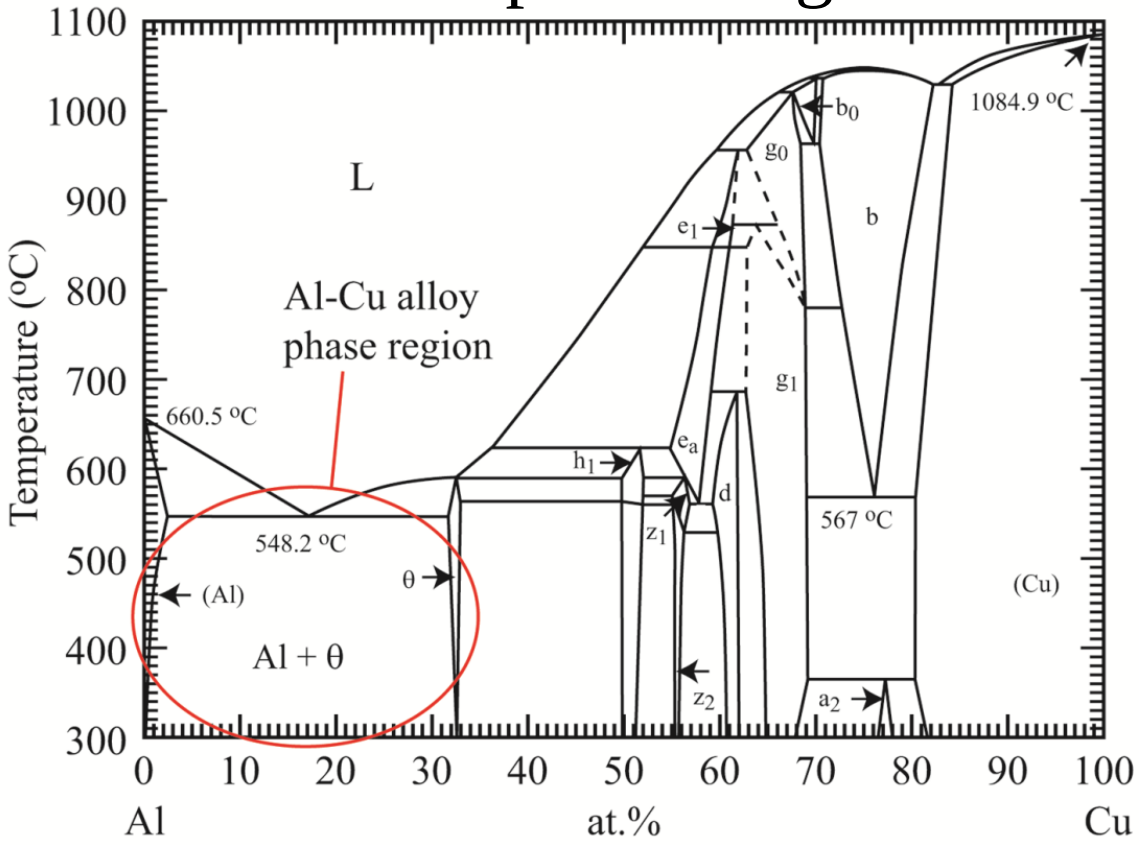

Cu solubility in Al

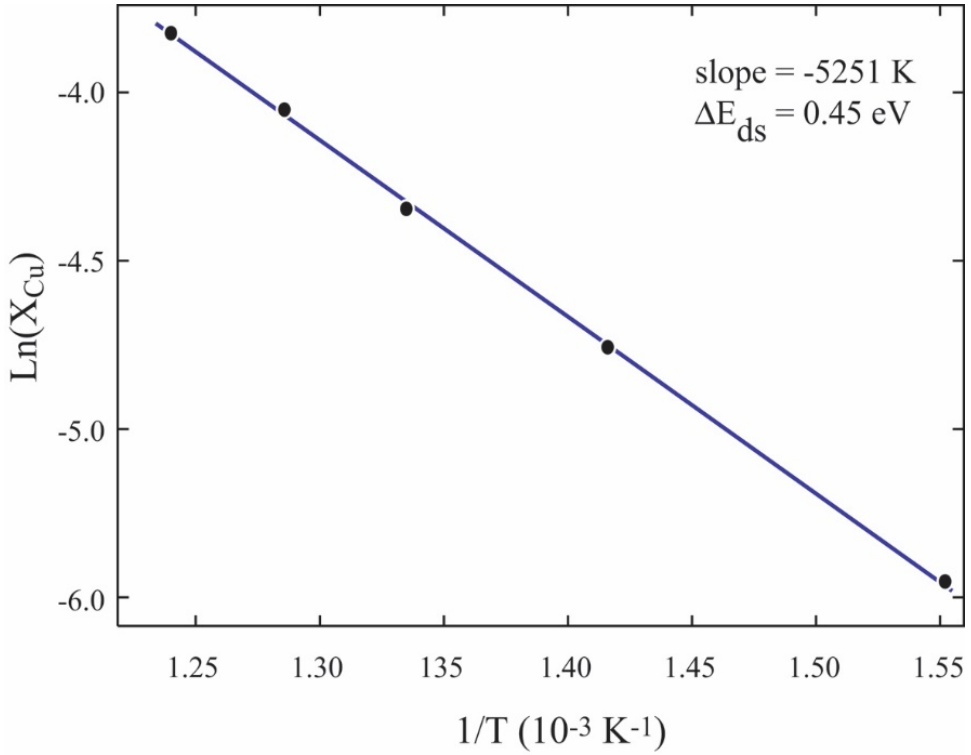

1. Traditionally, ΔE_{ds} of Cu in Al is for dissolving a Cu atoms
2. Should really be for dissolving Al_2Cu molecules

	ΔE_{ds} (eV)
ADP	1.09
EAM-CY	-0.06
BOP	0.14
DFT	0.40
Exp.	0.45

$H_2+H \rightarrow H+H_2$ chemical reaction

Hydrogen crystal to H_2 gas

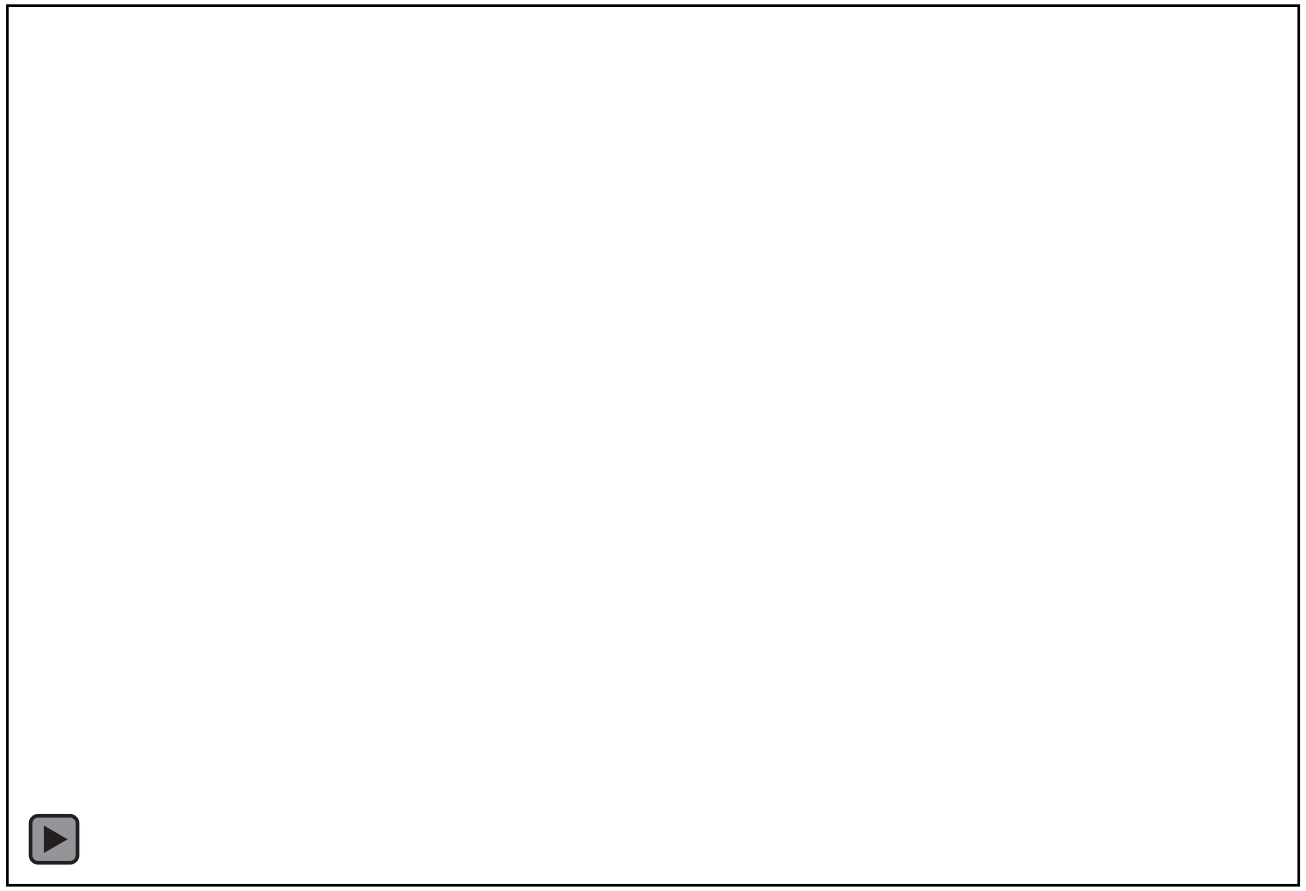

$H_2+H \rightarrow H+H_2$ energy profiles

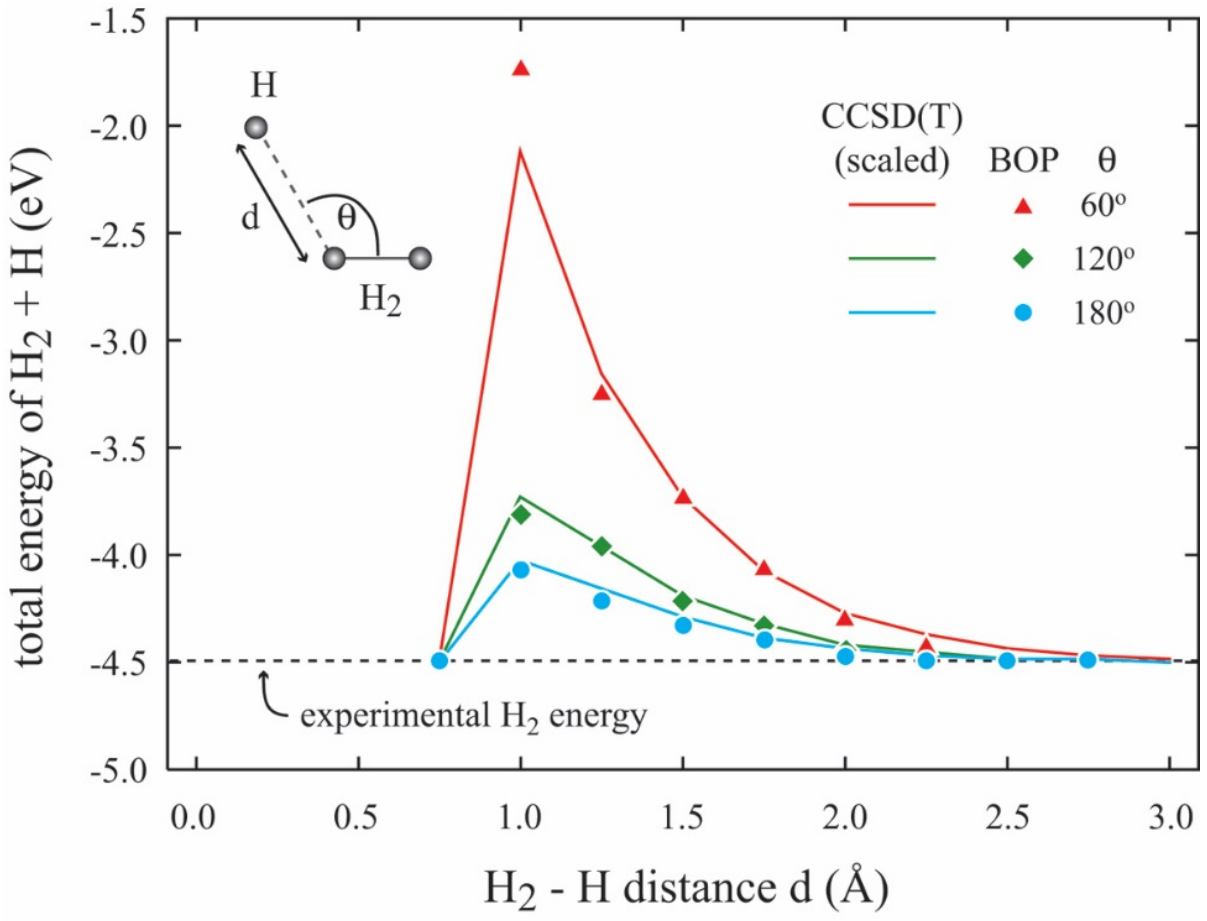

Al + H_2 and Cu + H_2 Phase Separation

(a) N_H/N_{Cu} = 0.20 with all atoms shown

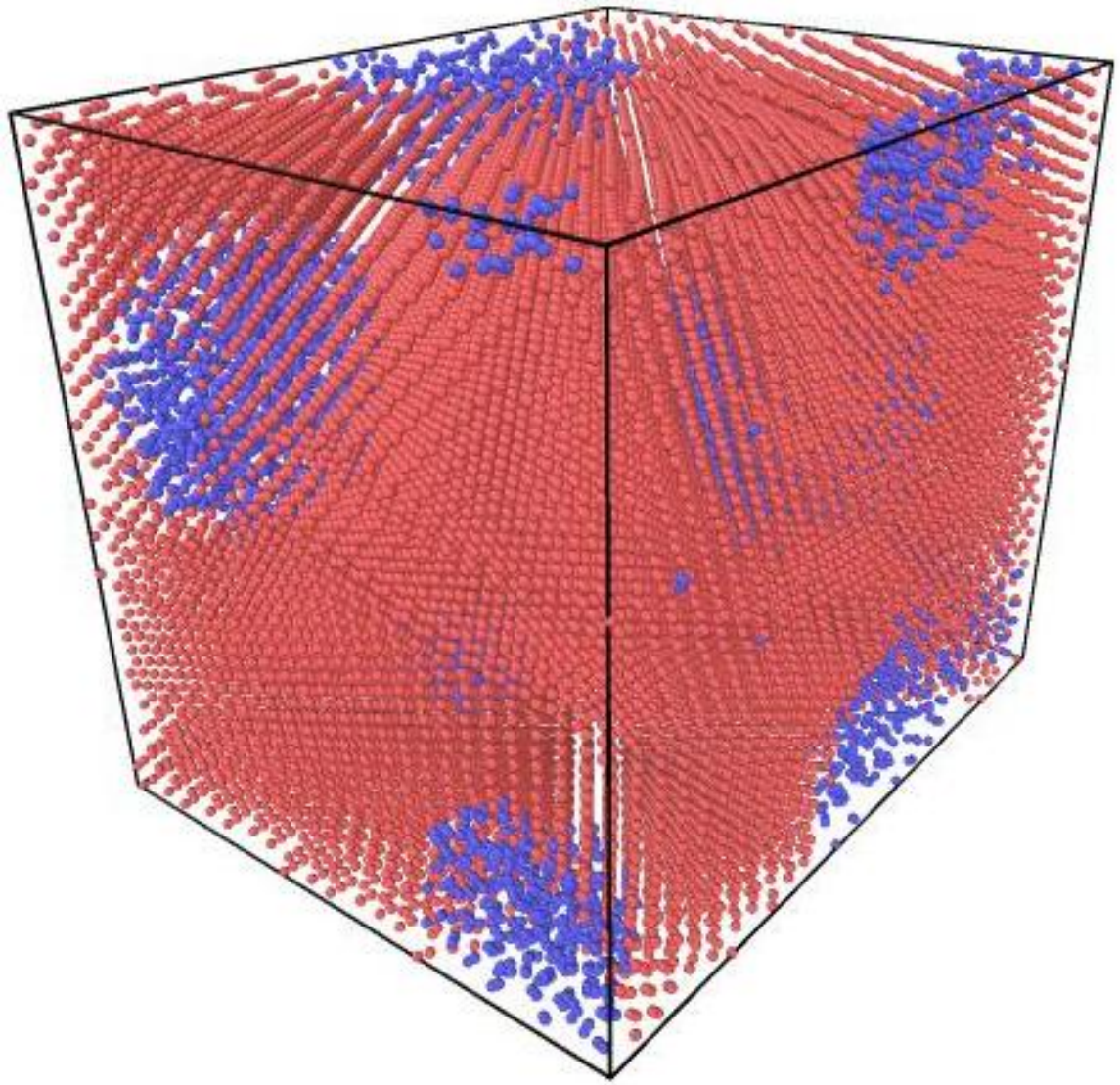

(b) only H atoms shown

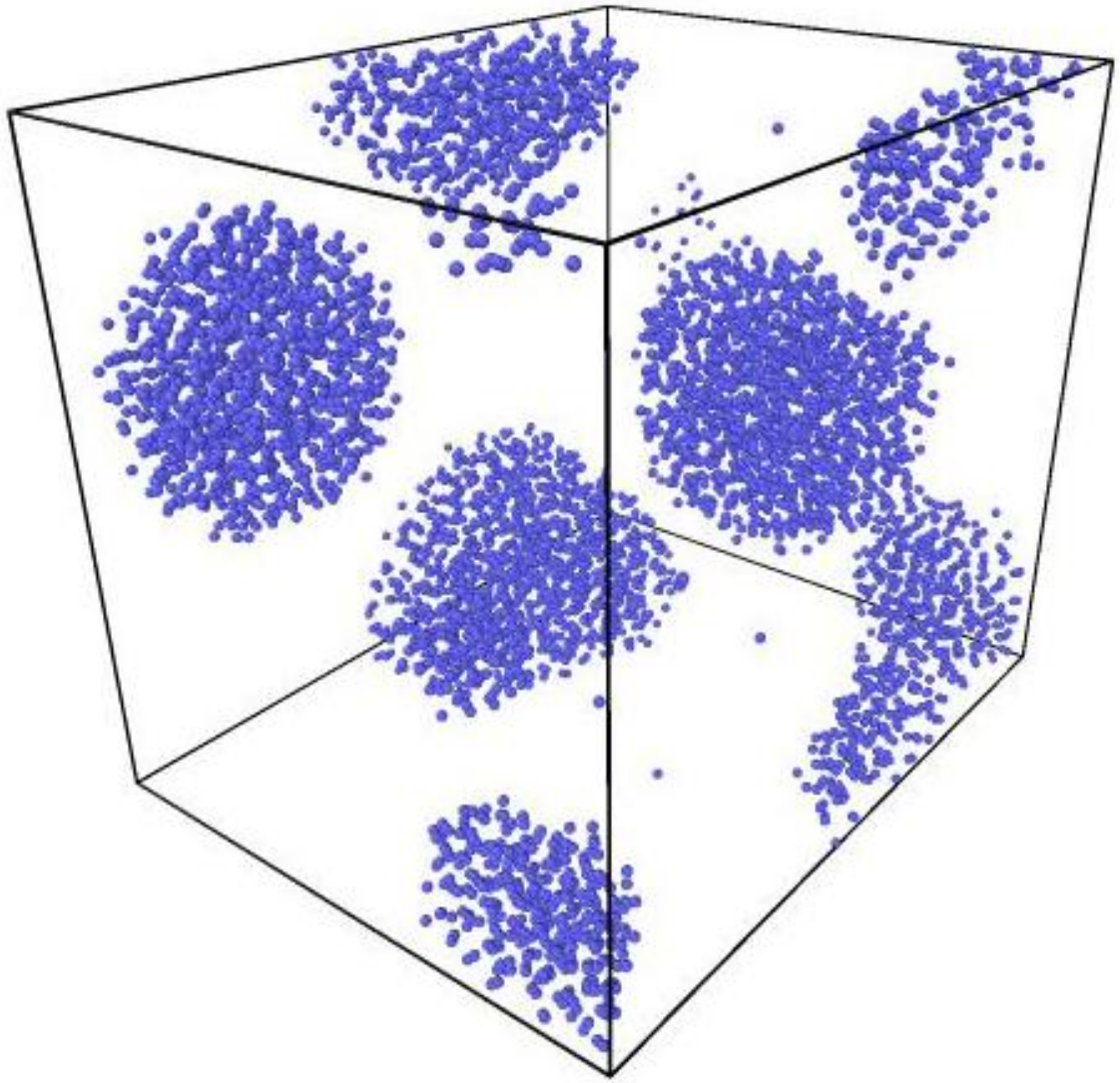

MD simulations of θ and θ' growth

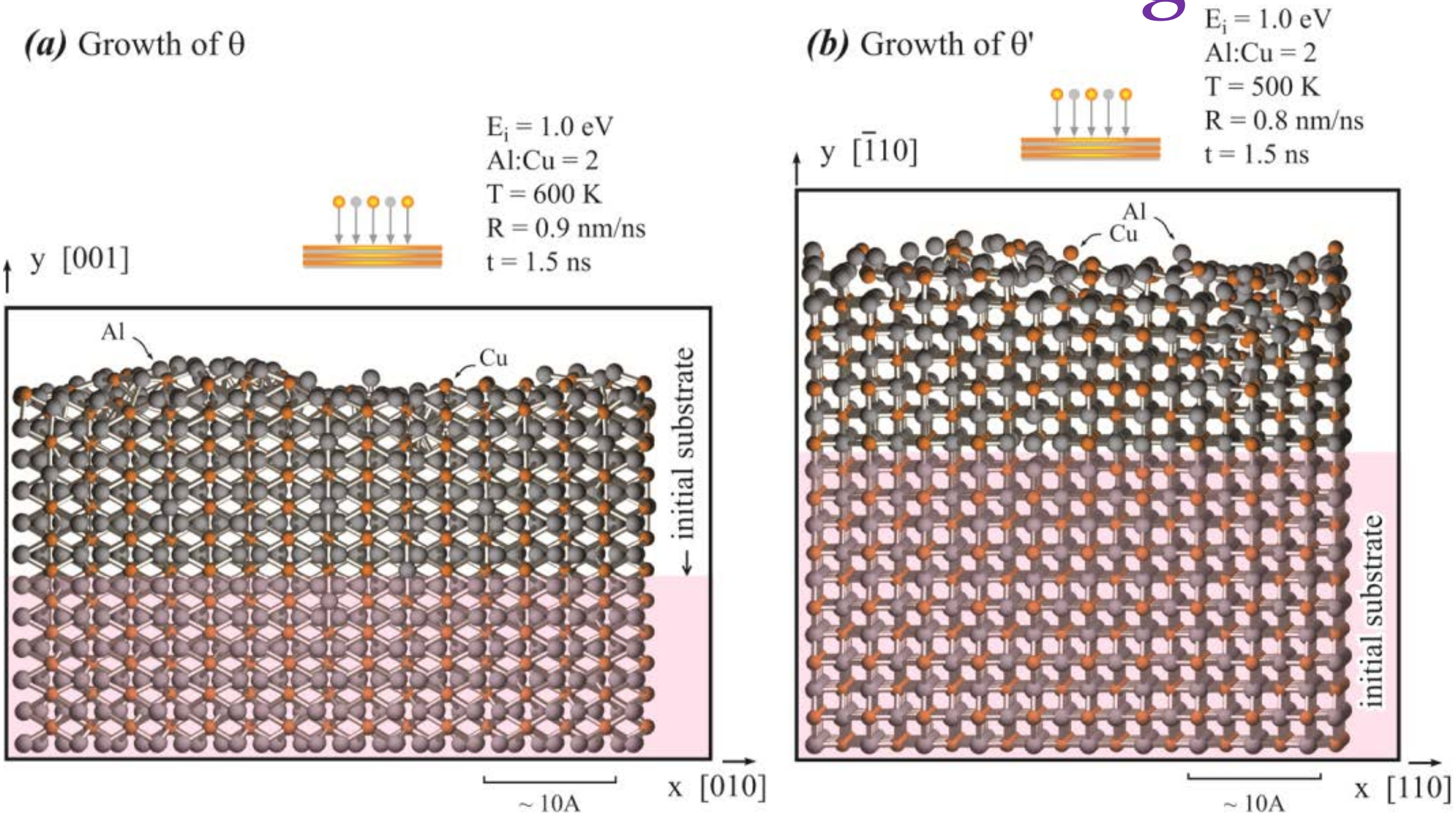

MD simulations H_2 absorption

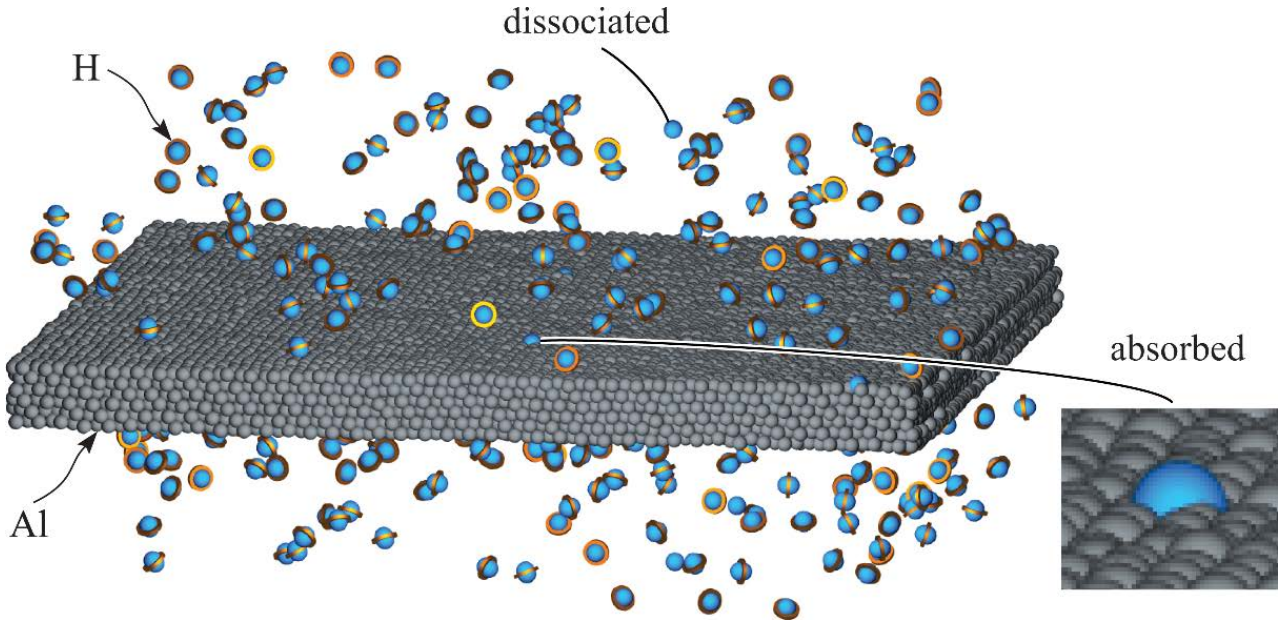

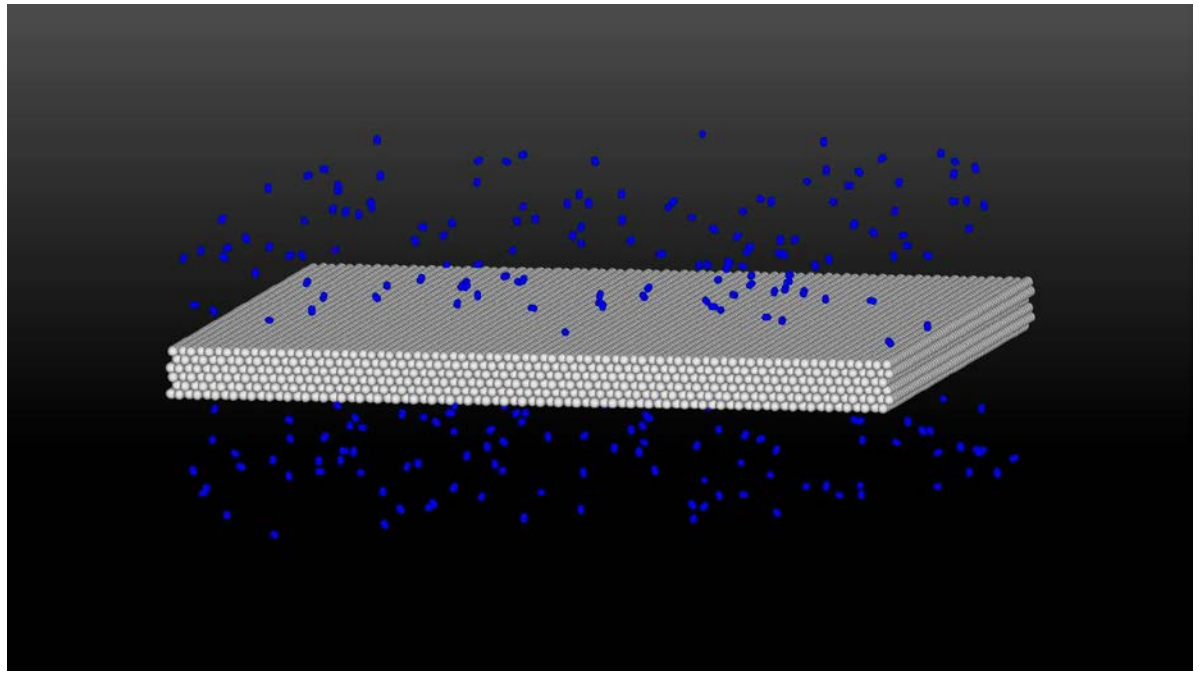

Such simulations are not possible without capturing the $H + H_2 \Leftrightarrow H_2 + H$ reaction.

Conclusions

1. Advanced potentials enable simulations of chemical reactions
2. Ensuring the stability of the equilibrium phase is challenging
3. Simple potentials easily capture the equilibrium phase
4. Traditional potential parameterizations target at specific properties important to the applications
5. New potential parameterization based on machine learning needs to incorporate traditional ideas